nature plants

ARTICLES

PUBLISHED: 4 APRIL 2016 | ARTICLE NUMBER: 16031 | DOI: 10.1038/NPLANTS.2016.31

State transitions redistribute rather than dissipate energy between the two photosystems in *Chlamydomonas*

Wojciech J. Nawrocki[1‡], Stefano Santabarbara[2‡], Laura Mosebach[1†], Francis-André Wollman[1*] and Fabrice Rappaport[1§]

Photosynthesis converts sunlight into biologically useful compounds, thus fuelling practically the entire biosphere. This process involves two photosystems acting in series powered by light harvesting complexes (LHCs) that dramatically increase the energy flux to the reaction centres. These complexes are the main targets of the regulatory processes that allow photosynthetic organisms to thrive across a broad range of light intensities. In microalgae, one mechanism for adjusting the flow of energy to the photosystems, state transitions, has a much larger amplitude than in terrestrial plants, whereas thermal dissipation of energy, the dominant regulatory mechanism in plants, only takes place after acclimation to high light. Here we show that, at variance with recent reports, microalgal state transitions do not dissipate light energy but redistribute it between the two photosystems, thereby allowing a well-balanced influx of excitation energy.

Oxygenic photosynthesis requires two photosystems, photosystem II (PSII) and I (PSI), acting in series to catalyse the transfer of electrons from water to CO_2. These two membrane-bound complexes convert light energy, by means of electron and proton transfer reactions, into electrochemical energy and ultimately into biologically useful free energy[1]. But before being converted, light energy must be captured, and the catalytic feat that these complexes achieve would be limited without the LHCs that increase the flux they sustain by more than two orders of magnitude funnelling light energy to the photochemical converters and thereby enhancing their absorption cross-section (reviewed in ref. 2).

Unsurprisingly, light harvesting is the major target of regulatory processes of photosynthesis[3]. In high light conditions, when the excitation flux exceeds the assimilation capacity, the limiting step of photosynthesis is one of the light independent electron transfer reactions, and regulatory mechanisms are triggered that decrease the excitation pressure and the resulting over-reduction of the electron acceptors, a potent source of light-induced damages. Prominent among these is non-photochemical quenching (qE), which increases the thermal dissipation of the excited state of chlorophylls[4].

In low light conditions, the turnover rate of each photosystem is proportional to the energy influx it receives and the least excited photosystem sets the velocity of the entire chain. Consequently, whereas a balanced excitation flux warrants a smooth operation in a dynamic range of light intensities, an unbalanced excitation influx generates a suboptimal oxidation state of the electron carriers in the chain and compromises its ability to cope with large and sudden changes in light intensity. This becomes critical in microalgae often exposed to hypoxic environmental conditions under which the plastoquinone pool that shuttles electrons between the two photosystems becomes over-reduced[5].

Since their discovery in microalgae in the late 1960s, 'state transitions' have been regarded as responsible for preserving a balanced excitation between the two photosystems[6,7] (reviewed in refs 8,9). State transitions involve the reversible phosphorylation of LHC antenna proteins and their consecutive lateral migration from the PSII-enriched stacked membrane regions of the thylakoid, to the PSI-enriched unstacked ones[10,11]. The reversibility of this redistribution relies on the interplay of a phosphatase and a kinase that is activated by the reduction of the plastoquinone pool sensed by the cytochrome b_6f complex (reviewed in ref. 8). Thus, in unicellular green algae, state transitions would adjust the relative antenna sizes of the two photosystems using the redox state of plastoquinones as a sensor of their uneven light excitation or of changes in light-independent metabolic processes that impact the redox state of the chloroplast stroma and, consecutively, of the photosynthetic electron transfer chain. In this view, the respective light harvesting capacity of each photosystem would change in a compensatory manner with the mobile LHC commuting between the two photosystems, not only to balance the excitonic flux but also to meet the cell's demand for ATP upon changes in environmental conditions[12].

Yet this view has been repeatedly challenged in the 1980s[13] and more recently in studies[14–17] that concluded that microalgae undergo state transitions of much larger amplitude than vascular plants because a major fraction of the mobile antenna detached from PSII remains disconnected from PSI and aggregated in a quenched state. Accordingly, green algae such as *Chlamydomonas reinhardtii* would be equipped with only one major regulatory mechanism dissipating energy, using both state transitions and qE under low and high light respectively, but there would be only a minor contribution of state transitions in balancing the excitation flux under low light conditions.

This is however hard to reconcile with the physiology of *Chlamydomonas* found on soil and in shallow ponds, where light intensities are rarely excessive but are prone to generating hypoxic conditions, as documented by a metabolic flexibility that plants do not develop[18]. This idiosyncratic feature calls for a preserved photosynthetic activity to keep high levels of intracellular ATP

[1]Institut de Biologie Physico-Chimique, UMR 7141 CNRS-UPMC, 13 rue P. et M. Curie 75005, Paris, France. [2]Istituto di Biofisica, Consiglio Nazionale delle Ricerche, Via Celoria 26, 20133 Milan, Italy. [†]Present address: Munster University, Institute of Plant Biology & Biotechnology, D-48143 Muenster, Germany. [‡]These authors contributed equally to the work. [§]Deceased. *e-mail: francis-andre.wollman@ibpc.fr

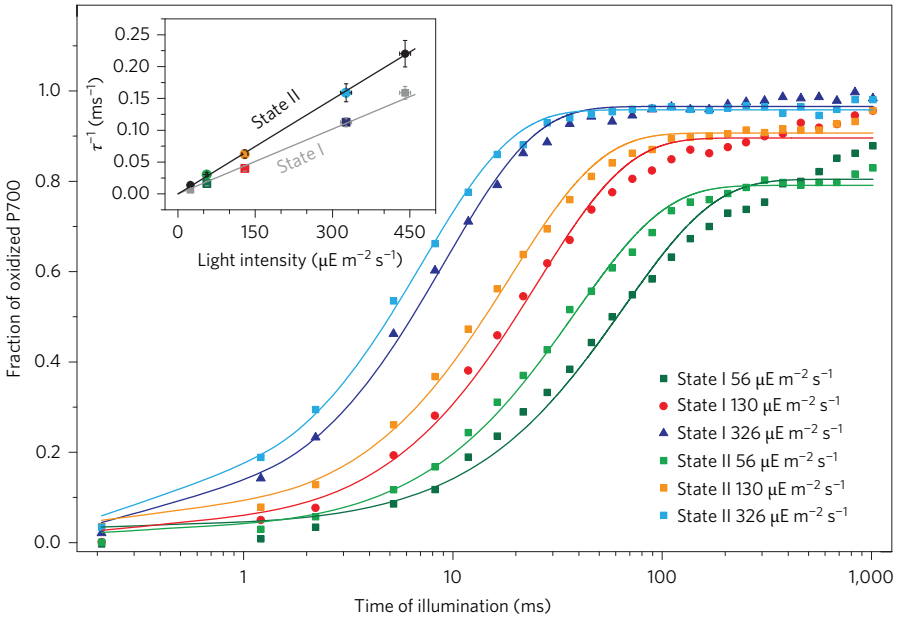

Figure 1 | Kinetics of P700 oxidation in a ΔPC *C. reinhardtii* mutant. The light-induced oxidation of the P700 dimer of PSI chlorophylls was recorded at 705 nm. Experimental data are shown as symbols and the solid lines are monoexponential fits of oxidation kinetics. These were measured at different light intensities in both state I and state II. The inset shows the linear dependence of the oxidation rate determined by the monoexponential fit on the light intensity in both state I and state II. The ratio between the two slopes yields the change in the PSI antenna size upon state transitions (1.4 ± 0.1). The data shown in the inset are the average of $n = 13$ independent biological replicates.

when the plastoquinone pool is reduced in the dark in response to hypoxic/anoxic conditions, and it also rationalizes the inability of *Chlamydomonas* to develop a qE-type of quenching unless acclimated to high light beforehand[19].

The paradoxical conclusions conflicting with the ecology of green microalgae, such as *Chlamydomonas*, which have attracted huge biotechnological interest owing to the potential of their metabolic plasticity, prompted us to reassess the mechanism of state transitions in this unicellular model organism.

Results

We first sought a direct method to measure the PSI antenna size and its putative relative change upon state transitions. We reasoned that measuring the oxidation rate of P700 in a mutant lacking plastocyanin (ΔPC) meets this purpose because, in such a mutant, each charge separation generates a long-lived $P700^+$ because of the absence of a secondary donor. Thus the rate of formation of $P700^+$ in continuous light is determined by the rate at which PSI is excited, which is proportional to the antenna size and to the light intensity. Such a mutant however prevents the tight control of the redox state of the plastoquinone pool and thus the achievement of a complete state I. Indeed, in the absence of PC, the plastoquinone pool cannot be fully oxidized by illumination and inhibition of PSII, owing to the interruption of the chain upstream of PSI. State I conditions were thus promoted by a vigorous aeration of the cells in darkness, a method that has been reported previously to produce up to 80% of the completion of state I (refs 20,21). State II was achieved by placing the cells in anoxia, as in refs 15,16.

Figure 1 shows the kinetics of the light-induced absorption changes at 705 nm with increasing light intensities in both state I and state II conditions. As shown in the inset, the oxidation rate of P700 , determined by fitting the oxidation kinetics with one exponential, increased linearly with the light intensity. Saliently, the slope of this linear plot increased by 39 ± 10% ($n = 13$) when there was a shift from state I to state II (inset of Fig. 1 and Fig. 2). We note that, whereas a single exponential yielded an excellent fit in state II, using two exponentials increased the quality in state I (see Supplementary Fig. 1). Interestingly, according to the bi-exponential fit, in state I the fast component accounted for ~20% of the total amplitude and was 1.4-fold faster than the slower component, which, in its turn, had a similar rate to that found in state II. This suggests that in the state I conditions we used with this mutant, ~20% of the mobile LHC is already bound to PSI in a state II configuration.

We next examined how the relative weight of the two components contributing to the P700 oxidation kinetics evolved as state transition took place. We globally fitted the series of individual kinetics measured during the time course of state transitions with a sum of two exponentials. We found that the relative amplitude of the fastest component progressively increased at the expense of the other one within 3 min after the induction of the state transitions (Fig. 3), consistent with previous reports on the rate of state transitions[22]. Accordingly, state transitions would involve a transient mixture of two types of PSI, having a 'state-I-like' and a 'state-II-like' antenna, rather than the progressive increase in the absorption cross-section of each individual PSI.

We then asked how these changes in PSI antenna size compare with the simultaneous variations in PSII antenna size. These variations are commonly assessed by measuring the change in fluorescence intensity under conditions where PSII photochemical traps are 'closed' (F_{max}), that is, they are unable to generate a stable radical pair[20]. At F_{max}, the emission is dominated by PSII and its intensity is proportional to the probability that a photon is absorbed by PSII. We thus measured in parallel to the P700 oxidation kinetics, that is with the same sample and in the same conditions, the decrease in F_{max} associated with the transition to state II in the ΔPC mutant. We found a decrease of 35 ± 5% (Fig. 2), which is similar to the 39 ± 10% increase estimated above for the change in the relative antenna size of PSI. However, to assess the complementarity of these changes in antenna, one needs to know the antenna size of PSII relative to that of PSI before the transition takes place.

We thus assessed the relative cross-section of PSII and PSI using the electrochromic shift (ECS) undergone by carotenoids and chlorophylls *b* bound to LHC proteins[23]. The absorption changes resulting from this shift are proportional to the transmembrane electric

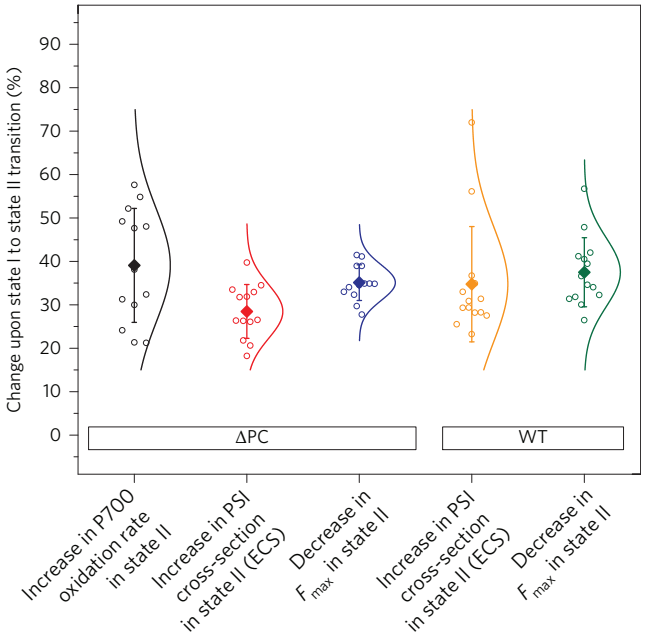

Figure 2 | Comparison of the changes in the PSII and PSI antenna size on state I to state II transitions using different approaches as detailed in the main text. The open symbols show the results of individual experiments, the filled symbols are the average $n \geq 13$ of biological replicates and the vertical lines show the standard deviations. The bell-shaped curves show the corresponding Gaussian distributions to illustrate the statistical scatter and the consecutive requirement for numerous biological replicates.

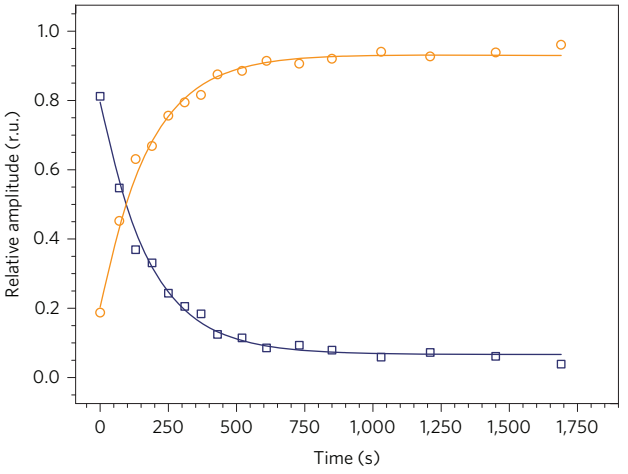

Figure 3 | Evolution, as a function of the time after induction of state transitions, of the fast and slow components in the oxidation kinetics of P700 in the ΔPC mutant. The sample was initially placed in state I, and then anoxia was induced at $t = 0$. Oxidation kinetics of P700 were measured at discrete time points following the induction of the transition to state II. They were globally fitted with two exponentials, leaving both the amplitude and life time as free running parameters. The fit yielded two components with respective time constants of 8.7 ± 0.1 ms (blue squares) and 5.9 ± 0.2 ms (orange circles); note that the ratio between the two is 1.4. The time course of the changes of the relative amplitudes of these two components as state transitions develop is shown and the overall time constant of the process was found to be 176 ± 10 s. Each single point is the average of three biological replicates at one light intensity. r.u., relative units.

field generated by photochemical charge separations. The ECS signal induced by a saturating and single turnover flash is thus proportional to the total number of charge separations undergone by all photosystems (I and II). Upon inhibition of PSII by specific inhibitors, the contribution of PSI alone and, after subtraction, that of PSII, can be determined. We thereby found that the PSII to PSI ratio per electron transfer chain was ~1 (Table 1). When using a weak, sub-saturating exciting flash, the probability that a given photosystem undergoes charge separation is determined by the probability that it traps an absorbed photon. Thus, when measured under non-saturating conditions, the ECS signal associated with PSI and PSII is proportional to their respective antenna size. In the ΔPC mutant, we found the ratio between the PSI and PSII absorption cross-section to be 1.2 ± 0.1 ($n = 7$) in state I (Table 1), which is consistent with the relative amplitude of the fast component in the P700 oxidation kinetics in state I (Fig. 3). It also is in perfect agreement with previous photoacoustic measurements with a dark-adapted wild-type (WT) strain[20].

When assessing the change in the relative absorption cross-section of PSI upon state transition using ECS, we found that it increased by 28 ± 5% (see Fig. 2). Although far from being negligible, this change is smaller than that estimated by the direct measure of the P700 oxidation rate. This apparent discrepancy between the ECS and P700 oxidation methods is readily explained by our above observations that a fraction of phosphorylated LHCII is already bound to PSI in state I conditions in the ΔPC mutant. Indeed, although the latter method leads to the complete oxidation of P700 and thus probes the entire population of PSI, the former method, relying on sub-saturating single turnover flashes, only probes a fraction of the PSI centres. In state I this fraction will be enriched in those PSI centres having the larger absorption cross-section and the method will overestimate the antenna size of PSI in state I, in turn underestimating the cross-section increase on transition to state II.

We then studied state transitions in the WT strain, grown in photoautotrophic conditions. Complete state I was achieved by fully oxidizing the plastoquinone pool by means of illumination in the presence of DCMU (3-(3,4-dichlorophenyl)-1,1-dimethylurea) to inhibit PSII. State II was promoted as for the ΔPC mutant, by anoxia. The more pronounced state I achieved with the WT relative to that in the ΔPC mutant resulted in larger changes in 77 K emission spectra, a method which is routinely used to assess state transitions[24] (see Supplementary Fig. 2).

Table 1 | The relative antenna size ± standard deviation of PSI and PSII in the WT and ΔPC.

	ΔPC (dark, oxic)	WT (DCMU, light, oxic)
PSI:PSII antenna size ratio in state I	1.2 ± 0.1 ($n = 7$)	1.0 ± 0.1 ($n = 9$)
PSI:PSII ratio	0.9 ± 0.1 ($n = 7$)	1.0 ± 0.1 ($n = 4$)

n is the number of biological replicates.

Using the ECS method described above, we found that the relative absorption cross-section of PSI with respect to PSII in state I was 1.0 ± 0.1 ($n = 9$; Table 1). With the same method, we found a 35 ± 9% ($n = 14$) increase in the PSI absorption cross-section when state transitions were completed from state I to state II. This is to be compared with a decrease of 38 ± 6% ($n = 14$) in PSII antenna size as assessed by the changes at F_{max}. Given this remarkable complementarity of the changes in antenna size of the two photosystems in the WT strain of *Chlamydomonas*, we conclude that virtually all of the peripheral antenna that detaches from PSII upon transition to state II functionally couples to PSI.

The present data fully support a redistribution of the light harvesting antenna between the two photosystems upon state transitions in *Chlamydomonas*, but conflict with any significant contribution of the aggregation-quenching LHCII model that has been recently proposed. To further re-assess the two models, we revisited the situation in a mutant lacking the PSI reaction centres.

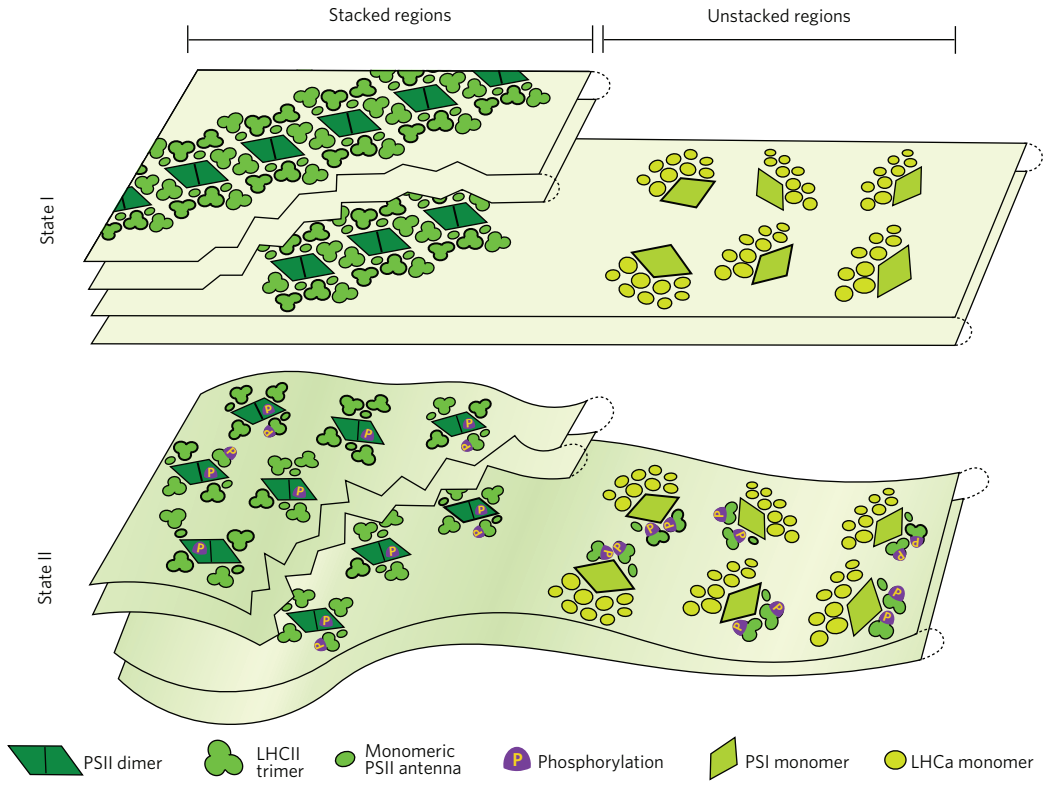

Figure 4 | A quantitative schematic of photosystem and antenna distribution heterogeneity, and of its change during state transitions, in *C. reinhardtii*. In state I, when the plastoquinone pool is oxidized, PSII-(3/4) LHCII supercomplexes form semi-crystalline arrays in the stacked regions of the thylakoids[43,44], whereas PSI form supercomplexes with nine LHCa proteins[45] mostly in the unstacked regions[11]. The functional antenna size of these photosystems is identical when plastoquinone pool is fully oxidized (this study). Upon reduction of the plastoquinone pool, phosphorylation of PSII core and antenna occurs, leading to electrostatic repulsion from the stacked regions of the membrane[13,46] and their migration to the unstacked regions[10,20], loosening the overall stacking[16]. In state II, the PSI-9 LHCa supercomplex further increases its size by about 40% (this article) by attaching two LHCII trimers and a monomeric antenna such as CP26/CP29 or 5 antenna subunits[28,29,33,47].

This mutant is predicted to have opposite behaviours on transition to state II depending on the model one considers. The 'antenna redistribution model' would predict no changes in F_{max}, because of the absence of the quenching sites provided by PSI. The 'aggregation-quenching model' would predict the same extent of decrease in F_{max} as in the WT, the quenching being independent of PSI. In agreement with the 'antenna redistribution model' we observed no quenching at F_{max} in this mutant on transition to state II, in line with Delosme *et al.*[20]. We checked that the unchanged F_{max} was not due to the lack of phosphorylation of the antenna protein that expectedly displayed the characteristics of state II in the ΔPSI mutant (see Supplementary Fig. 3). Thus PSI must be present to promote the quenching of fluorescence in state II, consistent with earlier conclusions that the absence of PSI in *Chlamydomonas*[20] or the lack of specific PSI subunits in PSI of *A. thaliana*[25] impeded state transitions.

Discussion

In unicellular green algae, state transitions (Fig. 4) have long been considered as a mechanism balancing the excitation flux of PSII and PSI by the shuttling of a mobile fraction of the antenna. However, this view has been repeatedly challenged (see ref. 13). Recent reports[14–17] have concluded that unique features of state transitions exist in the microalga *Chlamydomonas* that would develop self-quenching of its antenna proteins when placed in state II conditions. Contrarily to these statements, we have demonstrated with the present data that state transitions induce complementary variations of the antenna size of the two photosystems in *Chlamydomonas* and thus rebut the conclusions that a major fraction of the phosphorylated LHCII detached from PSII does not attach to PSI.

We used a plastocyanin-lacking mutant that allows the measurement of the PSI antenna size and of the homogeneity of the absorption cross-section of the PSI population. This mutant, despite having the drawback of not allowing a full state I to be achieved, also provided a picture of the dynamics of the transient homogeneity/heterogeneity of the PSI antenna during state transitions. We observed that the absorption cross-section of PSI increases significantly on transition to state II, and that this increase is commensurate to the decrease in the PSII antenna. An alternative approach relying on ECS measurements provided additional support by evidencing, in the ΔPC mutant and in the WT strain grown under photoautotrophic conditions, the complementary redistribution of the respective antenna of the two photosystems by 35–40%. Last, the absence of fluorescence quenching at F_{max} in state II conditions when using a PSI-lacking mutant showed that PSI is required to trap the excitation of phospho-LHCII detached from PSII.

As regards to the assessment of the PSII antenna from F_{max} data at room temperature, a reliable determination of the variation in the number of chlorophylls connected to PSII requires taking into account the small but not completely negligible contribution of the PSI photochemical units to the overall fluorescence emission. It has been estimated as 15–30% of F_0 (ref. 26) which in *C. reinhardtii* typically has an F_0/F_{max} ratio of 0.3, leading to a contribution of PSI to F_{max} of ~5–10% at the relevant detection wavelength[27]. Thus the variations of F_{max} by 35% and 39% in the ΔPC and WT strains correspond to changes in the PSII antenna size of 37–39% and 41–43%, respectively.

Table 2 | A summary of the stoichiometry of chlorophylls in the photosystems and LHCs.

Chlamydomonas reinhardtii	PSII (monomer)	PSI	PSI/PSII antenna size
A | State I			
Core size	35 chls[48]	97 chls[49]	1 ± 0.1 (this work)
Antenna pool size	~3–4 LHCII trimers = 126–168 chls + CP26, CP29 = 26 chls[44,50]	9 LHCI ≈ 126 chls[45]	
Total size	~190–230 chls	~220 chls	
B | Oxic, darkness (incomplete state I)			
Total size	~210 chls	~250 chls	1.2 ± 0.1 (this work and ref. 20)
C | State II			
Core size	35 chls[48]	97 chls[49]	2.35 (this work)
Antenna pool size	~2 LHCII trimers = 84 chls CP26/CP29 = 13 chls (ref. 44 and this work)	~9 LHCI ≈ 126 chls[45] + ~2 LHCII trimers = 84 chls CP26/CP29 = 13 chls[28] or ~2 LHCbM5 + ~2 CP29 + ~1 CP26 = 70 chls[29]	
Total size	~135 chls	~300–320 chls	
D | Percentage of change upon state transitions (this work)			
From state I to state II	–42 ± 6%	+35 ± 9% (ECS)	-
From incomplete state I to state II	–38 ± 5%	+39 ± 10% (P700 oxidation)	
Mobile chls	2 LHCII trimers + CP26/CP29[28,45] = 97 (46%) 5 antenna subunits[29] = 70 (33%)		

The information presented here compares current knowledge from the literature regarding *C. reinhardtii* with the conclusions drawn from the present study.

But is the present finding that about 35–40% of antenna moves between PSII and PSI on state transitions quantitatively compatible with the current knowledge on the biochemical and pigment contents of this mobile antenna? These data, available from the literature, are recapped in Table 2.

According to the literature, in *C. reinhardtii*, PSII bears 190–230 (a conservative figure of 210 will be used hereafter) chlorophylls in state I and PSI 220 (see Table 2) Consistent with this, we found that PSI and PSII have similar antenna size in the WT in state I. In the ΔPC mutant, the antenna size of PSI relative to PSII was 1.2 and this is explained by the incomplete oxidation of the plastoquinone pool in the experimental conditions used to generate state I. Therefore, assuming no disconnected chlorophylls and neglecting the slightly smaller trapping efficiency of PSII versus PSI (because, considering the intrinsic scatter of biological data, this would be a second order correction), the antenna size would be 195 chls (chlorophylls) for PSII and 235 chls for PSI in state I in this strain. With this in mind and considering the biological and experimental uncertainties of these figures, the 38% decrease in PSII antenna size in the ΔPC mutant would involve the disconnection of ~75 chls from PSII that when bound to PSI would result in a 33% increase in its absorption cross-section, in reasonable agreement with the 39% found here. As to the WT, the 42% decrease in the PSII antenna size corresponds to the detachment of ~85 chls, which also matches the 35% complementary increase of the PSI absorption cross-section.

These estimates also fall in line with refs 28,29 which characterized the LHCII–LHCI–PSI supercomplexes isolated from state II conditions. They contained—apart from the constitutive nine LHCI and the core—two LHCII trimers and a monomeric peripheral antenna[28] or five antenna subunits[29]. In terms of chlorophyll per photosystem, this adds 97 or 70 chls, which, assuming identical efficiency for the energy transfer to the core as from the LHCI chlorophylls[30,31] translates into a 33–46% increase in the antenna size compared with state I, in good agreement with our results (39–44%). Importantly, it means that in complete state II, *all* the PSI–LHCI supercomplexes bind at least two phospho-LHC trimers.

Owing to biological scatter and experimental errors (see the width of the Gaussian distribution in Fig. 2), we cannot definitely exclude the existence of a fraction of unbound LHCII in state II conditions but the present data show that it must be minor. A similar conclusion was also reached by Wlodarczyk *et al.*,[32] who reported, based on the study of the fluorescence emission lifetime at 77 and 6 K, the presence of a yet uncharacterized component emitting at 685 nm, that they assigned to unbound LHCII and which accounted for 20% of the mobile LHC pool, the remaining 80% being bound to PSI. According to our data, obtained at room temperature, the maximum fraction of disconnected and quenched LHC would be closer to 10% and the possibility remains that structural modifications induced by freezing of the thylakoid membranes in low temperature measurements led to an overestimation of the detached LHCII pool.

Thus, as depicted in Fig. 4, we found that in state II, in *C. reinhardtii*, the vast majority of PSI centres bind 2 LHCII trimers and probably another monomeric antenna[33]. The increase in PSI antenna size agrees well with biochemical and structural data and so does the complementary decrease in that of PSII. The extent of state transitions in microalgae is therefore higher than in vascular plants, and contrary to those recent reports that suggested an LHCII aggregation-quenching process[14–16] (see Supplementary Information for further discussion), it consists mostly of photochemical quenching by PSI. The antenna redistribution model fits well with the ecological niche the algae inhabit, *Chlamydomonas* being often exposed to hypoxic or anoxic conditions when growing on soil in dense populations[18], conditions that are never met by land plants. This habitat also results in low light exposure and in the presence of reduced carbon sources from the microbial environment. The physiology of state transitions is then to increase the photochemistry of PSI to compete more efficiently with both photochemical and non-photochemical reduction of electron carriers—the latter being

important in algae because of a different sugar metabolism in the chloroplast and an increased rate of chlororespiration[5,34]. Consistent with this, a *Chlamydomonas* mutant having impaired respiration, and thus an over-reduced stroma in the dark, shows impaired growth in light-limiting conditions when unable to perform state transitions[12]. Indeed, the increased PSI antenna size in state II conditions, combined with the induction of the hydrogenase, ensures an efficient recovery from over-reducing conditions in hypoxia/anoxia—allowing rapid restoration of linear and cyclic electron flows, a critical issue for algal survival in its natural habitat[35,36].

Methods

Strains, growth conditions and treatments. *Chlamydomonas reinhardtii* strains used in this study are WT and mutant progeny from a cross between a plastocyanin lacking mutant ac208 (ref. 37) and a control strain from our laboratory, both derived from the original WT 137-C. These strains therefore are in a similar genetic background[38]. The WT was grown in photoautotrophic conditions in Minimum medium[18] under moderate light (30 μE m^{-2} s^{-1}). ΔPC was grown in heterotrophic conditions, in TAP medium[18] containing acetate as a reduced carbon source, at 30 μE m^{-2} s^{-1}. Cells were harvested in mid-log phase (1–4 × 10^6 cells ml^{-1}), concentrated approximately sixfold in Minimum medium supplemented with Ficoll 400 (10% w/w) and shaken in darkness in open flasks at 300 rpm for at least 30 min before measurements were taken. To induce state II, glucose (20 mM) and glucose oxidase (50 U ml^{-1}; type II, from *A. niger*) were used. State I conditions were achieved by light-DCMU (10 μM) treatment (WT) or by vigorous shaking in the dark (ΔPC). As a control strain unable to perform state transitions, we used the stt7-9 strain[12] which lacks the kinase responsible for the phosphorylation promoting the transition from state I to state II. As a mutant lacking PSI, we used a strain deleted for the *psaB* gene, which encodes one of the two main subunits of the core of PSI (ref. 39).

Time-resolved absorption spectroscopy. Light-induced absorption changes were measured as previously described in refs 40,41, with a JTS 10 (BioLogic) spectrophotometer that uses pulsed LED for detecting light sources. The appropriate detection wavelengths were selected using interferences filters: 705 nm, 10 nm full width at half maximum (FWHM) to measure the oxidation kinetics of P700, 520 nm, 10 nm FWHM and 546 nm, 10 nm FWHM to measure the ECS absorption changes. LEDs (emitting 640 nm) were used as continuous exciting light source. Single turnover flashes were provided by a dye laser (DCM, Exciton dye laser) pumped by a frequency doubled Nd:YAG Laser (Minilite II, Continuum). Actinic light was filtered by a 3 mm thick RG695 Schott glass filters when detecting at 705 and 3 mm BG39 Schott filters when detecting at 520 and 546 nm. The ECS absorption changes were determined after subtraction of the absorption changes measured at 546 nm to those measured at 520 nm.

Because DCMU (10 μM) was used systematically in the WT to achieve a complete state I, this PSII inhibitor was also added to the ΔPC strain when measuring the oxidation of P700 for the sake of consistency. In addition, hydroxylamine (10 mM) was added, when required, to cancel the contribution of PSII to the ECS signal measured after a single turnover flash. The mono- and biexponential fitting was done with OriginLab software. To check that the possible contribution of fluorescence changes to the signal measured at 705 nm were negligible, we checked that the P700 oxidation-induced absorption changes at 820 nm, where the contribution of fluorescence should be smaller, were in good agreement with those measured at 705 nm (see Supplementary Fig. 4).

Fluorescence spectroscopy. Fluorescence measurements were measured using the JTS 10 (Biologic) spectrophotometer in 'fluorescence' mode as described previously[26]. The fluorescence yield was probed using broad band blue detecting pulses. To warrant homogeneous illumination throughout the sample, green light was used as an actinic light (peak emission at 530 nm, FWHM 50 nm). The detecting and actinic light was filtered using a combination of a long pass reflecting filter (50% transmission at 650 nm) and an RG665 Schott filter. The samples were poisoned with 10 μM DCMU before the experiments to maintain the PSII centres at F_{max} in both oxic and anoxic conditions.

77 K fluorescence emission spectra. Low temperature emission spectra were measured using a laboratory built set-up. The samples, prepared as described above, were placed in an aluminium sample holder that was plunged into liquid nitrogen. The fluorescence exciting light was provided by a LED (λ_{max} 470 nm) and shone onto the sample using a Y-shaped optical fibre. The other branch of this fibre was connected to a CCD spectrophotometer (QE6500, Ocean Optics) to measure the emission spectrum.

Isolation of thylakoid membranes, western blotting and immunodetection with an anti-phosphothreonine antibody were performed as previously published[42].

Received 09 November 2015; accepted 16 February 2016; published online 4 April 2016

References

1. Archer, M. D. & Barber, J. *Molecular to Global Photosynthesis* (Imperial College Press, 2004).
2. Croce, R. & van Amerongen, H. Natural strategies for photosynthetic light harvesting. *Nature Chem. Biol.* **10,** 492–501 (2014).
3. Rochaix, J.-D. Regulation and dynamics of the light-harvesting system. *Annu. Rev. Plant Biol.* **65,** 287–309 (2014).
4. Goss, R. & Lepetit, B. Biodiversity of NPQ. *J. Plant Physiol.* **172,** 13–32 (2015).
5. Nawrocki, W. J., Tourasse, N. J., Taly, A., Rappaport, F. & Wollman, F. A. The plastid terminal oxidase: its elusive function points to multiple contributions to plastid physiology. *Ann. Rev. Plant Biol.* **66,** 49–74 (2015).
6. Bonaventura, C. & Myers, J. Fluorescence and oxygen evolution from *Chlorella pyrenoidosa*. *Biochim. Biophys. Acta* **189,** 366–383 (1969).
7. Murata, N. Control of excitation transfer in photosynthesis: Light-induced change of chlorophyll a fluorescence in porphyridium cruentum. *Biochim. Biophys. Acta* **172,** 242–251 (1969).
8. Wollman, F. A. State transitions reveal the dynamics and flexibility of the photosynthetic apparatus. *EMBO J.* **20,** 3623–3630 (2001).
9. Goldschmidt-Clermont, M. & Bassi, R. Sharing light between two photosystems: mechanism of state transitions. *Curr. Opin. Plant Biol.* **25,** 71–78 (2015).
10. Kyle, D. J., Staehelin, L. A. & Arntzen, C. J. Lateral mobility of the light-harvesting complex in chloroplast membranes controls excitation-energy distribution in higher-plants. *Arch. Biochem. Biophys.* **222,** 527–541 (1983).
11. Vallon, O., Wollman, F. A. & Olive, J. Lateral distribution of the main protein complexes of the photosynthetic apparatus in *Chlamydomonas-reinhardtii* and in spinach—an immunocytochemical study using intact thylakoid membranes and a PS-II enriched membrane preparation. *Photobiochem. Photobiophys.* **12,** 203–220 (1986).
12. Cardol, P. *et al.* Impaired respiration discloses the physiological significance of state transitions in *Chlamydomonas*. *Proc. Natl Acad. Sci. USA* **106,** 15979–15984 (2009).
13. Allen, J. F. Protein-phosphorylation in regulation of photosynthesis. *Biochim. Biophys. Acta* **1098,** 275–335 (1992).
14. Iwai, M., Yokono, M., Inada, N. & Minagawa, J. Live-cell imaging of photosystem II antenna dissociation during state transitions. *Proc. Natl Acad. Sci. USA* **107,** 2337–2342 (2010).
15. Unlu, C., Drop, B., Croce, R. & van Amerongen, H. state transitions in *Chlamydomonas reinhardtii* strongly modulate the functional size of photosystem II but not of photosystem I. *Proc. Natl Acad. Sci. USA* **111,** 3460–3465 (2014).
16. Nagy, G. *et al.* Chloroplast remodeling during state transitions in *Chlamydomonas reinhardtii* as revealed by noninvasive techniques *in vivo*. *Proc. Natl Acad. Sci. USA* **111,** 5042–5047 (2014).
17. Unlu, C., Polukhina, I. & van Amerongen, H. Origin of pronounced differences in 77 K fluorescence of the green alga *Chlamydomonas reinhardtii* in state 1 and 2. *Eur. Biophys. J.* http://dx.doi.org/10.1007/s00249-015-1087-9 (2015).
18. *The Chlamydomonas Sourcebook* 2nd edn (eds Harris, E. H., Stern, D. B. & Witman, G. B.) 1–24 (Academic Press, 2009).
19. Peers, G. *et al.* An ancient light-harvesting protein is critical for the regulation of algal photosynthesis. *Nature* **462,** 518–U215 (2009). .
20. Delosme, R., Olive, J. & Wollman, F. A. Changes in light energy distribution upon state transitions: an *in vivo* photoacoustic study of the wild type and photosynthesis mutants from *Chlamydomonas reinhardtii*. *Biochim. Biophys. Acta-Bioenerg.* **1273,** 150–158 (1996).
21. Houille-Vernes, L., Rappaport, F., Wollman, F. A., Alric, J. & Johnson, X. Plastid terminal oxidase 2 (PTOX2) is the major oxidase involved in chlororespiration in *Chlamydomonas*. *Proc. Natl Acad. Sci. USA* **108,** 20820–20825 (2011).
22. Delepelaire, P. & Wollman, F. A. Correlations between fluorescence and phosphorylation changes in thylakoid membranes of *Chlamydomonas-reinhardtii in vivo*—a kinetic-analysis. *Biochim. Biophys. Acta* **809,** 277–283 (1985).
23. Witt, H. T. Energy-conversion in the functional membrane of photosynthesis – analysis by light-pulse and electric pulse methods - central role of the electric-field. *Biochim. Biophys. Acta* **505,** 355–427 (1979).
24. Murakami, A. Quantitative analysis of 77K fluorescence emission spectra in *Synechocystis* sp. PCC 6714 and *Chlamydomonas reinhardtii* with variable PS I/PS II stoichiometries. *Photosynth. Res.* **53,** 141–148 (1997).
25. Lunde, C., Jensen, P. E., Haldrup, A., Knoetzel, J. & Scheller, H. V. The PSI-H subunit of photosystem I is essential for state transitions in plant photosynthesis. *Nature* **408,** 613–615 (2000).
26. Rappaport, F., Beal, D., Joliot, A. & Joliot, P. On the advantages of using green light to study fluorescence yield changes in leaves. *Biochim. Biophys. Acta* **1767,** 56–65 (2007).
27. Rizzo, F., Zucchelli, G., Jennings, R. & Santabarbara, S. Wavelength dependence of the fluorescence emission under conditions of open and closed Photosystem II reaction centres in the green alga *Chlorella sorokiniana*. *Biochim. Biophys. Acta-Bioenerg.* **1837,** 726–733 (2014).

28. Drop, B., Yadav, K. N. S., Boekema, E. J. & Croce, R. Consequences of state transitions on the structural and functional organization of photosystem I in the green alga *Chlamydomonas reinhardtii*. *Plant J.* **78,** 181–191 (2014).
29. Takahashi, H., Okamuro, A., Minagawa, J. & Takahashi, Y. Biochemical characterization of photosystem I-associated light-harvesting complexes I and II isolated from state 2 cells of *Chlamydomonas reinhardtii*. *Plant Cell Physiol.* **55,** 1437–1449 (2014).
30. Galka, P. *et al.* Functional analyses of the plant photosystem I-light-harvesting complex II supercomplex reveal that light-harvesting complex II loosely bound to photosystem II is a very efficient antenna for photosystem I in state II. *Plant Cell* **24,** 2963–2978 (2012).
31. Le Quiniou, C. *et al.* PSI-LHCI of *Chlamydomonas reinhardtii*: Increasing the absorption cross section without losing efficiency. *Biochim. Biophys. Acta* **1847,** 458–467 (2015).
32. Wlodarczyk, L. M. *et al.* Functional rearrangement of the light-harvesting antenna upon state transitions in a green alga. *Biophys. J.* **108,** 261–271 (2015).
33. Takahashi, H., Iwai, M., Takahashi, Y. & Minagawa, J. Identification of the mobile light-harvesting complex II polypeptides for state transitions in *Chlamydomonas reinhardtii*. *Proc. Natl Acad. Sci. USA* **103,** 477–482 (2006).
34. Johnson, X. & Alric, J. Interaction between starch breakdown, acetate assimilation, and photosynthetic cyclic electron flow in *Chlamydomonas reinhardtii*. *J. Biol. Chem.* **287,** 26445–26452 (2012).
35. Clowez, S., Godaux, D., Cardol, P., Wollman, F. A. & Rappaport, F. The involvement of hydrogen-producing and ATP-dependent NADPH-consuming pathways in setting the redox poise in the chloroplast of *Chlamydomonas reinhardtii* in anoxia. *J. Biol. Chem.* **290,** 8666–8676 (2015).
36. Godaux, D., Bailleul, B., Berne, N. & Cardol, P. Induction of photosynthetic carbon fixation in anoxia relies on hydrogenase activity and proton-gradient regulation-like1-mediated cyclic electron flow in *Chlamydomonas reinhardtii*. *Plant Physiol.* **168,** 648–658 (2015).
37. Quinn, J. *et al.* The plastocyanin-deficient phenotype of *Chlamydomonas reinhardtii* Ac-208 results from a frame-shift mutation in the nuclear gene encoding preapoplastocyanin. *J. Biol. Chem.* **268,** 7832–7841 (1993).
38. Gallaher, S. D., Fitz-Gibbon, S. T., Glaesener, A. G., Pellegrini, M. & Merchant, S. S. *Chlamydomonas* genome resource for laboratory strains reveals a mosaic of sequence variation, identifies true strain histories, and enables strain-specific studies. *Plant Cell* **27,** 2335–2352 (2015).
39. Redding, K. *et al.* A systematic survey of conserved histidines in the core subunits of Photosystem I by site-directed mutagenesis reveals the likely axial ligands of P-700. *EMBO J.* **17,** 50–60 (1998).
40. Joliot, P. & Joliot, A. Quantification of cyclic and linear flows in plants. *Proc. Natl Acad. Sci. USA* **102,** 4913–4918 (2005).
41. Alric, J., Lavergne, J. & Rappaport, F. Redox and ATP control of photosynthetic cyclic electron flow in Chlamydomonas reinhardtii (I) aerobic conditions. *Biochim. Biophys. Acta-Bioenerg.* **1797,** 44–51 (2010).
42. Takahashi, H., Clowez, S., Wollman, F. A., Vallon, O. & Rappaport, F. Cyclic electron flow is redox-controlled but independent of state transition. *Nature Commun.* **4,** 1954 (2013).
43. Engel, B. D. *et al.* Native architecture of the *Chlamydomonas* chloroplast revealed by *in situ* cryo-electron tomography. *eLife* **4** (2015).
44. Drop, B. *et al.* Light-harvesting complex II (LHCII) and its supramolecular organization in Chlamydomonas reinhardtii. *Biochim. Biophys. Acta* **1837,** 63–72 (2014).
45. Drop, B. *et al.* Photosystem I of *Chlamydomonas reinhardtii* contains nine light-harvesting complexes (Lhca) located on one side of the core. *J. Biol. Chem.* **286,** 44878–44887 (2011).
46. Barber, J. Regulation of energy-transfer by cations and protein-phosphorylation in relation to thylakoid membrane organization. *Photosynth. Res.* **10,** 243–253 (1986).
47. Kargul, J. *et al.* Light-harvesting complex II protein CP29 binds to photosystem I of *Chlamydomonas reinhardtii* under state 2 conditions. *FEBS J.* **272,** 4797–4806 (2005).
48. Suga, M. *et al.* Native structure of photosystem II at 1.95 A resolution viewed by femtosecond X-ray pulses. *Nature* **517,** 99–103 (2015).
49. Mazor, Y., Borovikova, A. & Nelson, N. The structure of plant photosystem I super-complex at 2.8 A resolution. *eLife* **4,** e07433 (2015).
50. Tokutsu, R., Kato, N., Bui, K. H., Ishikawa, T. & Minagawa, J. Revisiting the supramolecular organization of photosystem II in *Chlamydomonas reinhardtii*. *J. Biol. Chem.* **287,** 31574–31581 (2012).

Acknowledgements

We thank S. Bujaldon for the ΔPC-WT cross. W.J.N., F.-A.W. and F.R. acknowledge the support of CNRS and Université Pierre et Marie Curie. This work was supported by the Initiative d'Excellence programme from the French State (grant DYNAMO, ANR-11-LABX-0011-01) and by the programme PHC PROCOPE 2014 PROJET no. 30729YB. W.J.N. is a recipient of a PhD fellowship from the Université Pierre et Marie Curie. S.S. acknowledges the support from the DYNAMO ANR-11-LABX-0011-01 grant for travel. L.M. was a recipient of the Studienstiftung des Deutschen Volkes fellowship for her Master studies. Fabrice Rappaport deceased before final acceptance of this manuscript. His co-authors wish to acknowledge his remarkable contributions to our current understanding of photosynthesis regulations.

Author contributions

W.J.N., S.S., L.M. performed the experiments. F.-A.W. and F.R. conceived and designed the research. All of the authors discussed, analysed the data and wrote the paper.

Additional information

Supplementary information is available online. Reprints and permissions information is available online at www.nature.com/reprints. Correspondence and requests for materials should be addressed to F.A.W.

Competing interests

The authors declare no competing financial interests.